Bioorganic & Medicinal Chemistry 18 (2010) 590–596

Contents lists available at ScienceDirect

Bioorganic & Medicinal Chemistry

journal homepage: www.elsevier.com/locate/bmc

Synthesis and optimization of thiadiazole derivatives as a novel class of substrate competitive c-Jun N-terminal kinase inhibitors

Surya K. De [a], Vida Chen [a], John L. Stebbins [a], Li-Hsing Chen [a], Jason F. Cellitti [a], Thomas Machleidt [b], Elisa Barile [a], Megan Riel-Mehan [a], Russell Dahl [a], Li Yang [a], Aras Emdadi [a], Ria Murphy [a], Maurizio Pellecchia [a,*]

[a] Burnham Institute for Medical Research, La Jolla, CA 92037, USA
[b] Invitrogen Corporation, Invitrogen Discovery Services, 501 Charmany Drive, Madison, WI 53719, USA

ARTICLE INFO

Article history:
Received 22 September 2009
Revised 30 November 2009
Accepted 3 December 2009
Available online 11 December 2009

ABSTRACT

A series of thiadiazole derivatives has been designed as potential allosteric, substrate competitive inhibitors of the protein kinase JNK. We report on the synthesis, characterization and evaluation of a series of compounds that resulted in the identification of potent and selective JNK inhibitors targeting its JIP-1 docking site.

1. Introduction

The c-Jun N-terminal kinases (JNKs) were initially described in the early 1990s as a family of serine/threonine protein kinases, activated by a range of stress stimuli and able to phosphorylate the N-terminal transactivation domain of the c-Jun transcription factor.[1]

Three distinct genes encoding JNKs have been identified as JNK-1, JNK-2, and JNK-3, and at least 10 different splicing isoforms exist in mammalian cells.[2–4] The three JNK isoforms share more than 90% amino acid sequence identity and the ATP pocket is highly conserved (>98% identities). These proteins are activated in response to cellular stresses such as heat shock, irradiation, hypoxia, chemotoxins, and peroxides. They are also activated in response to various cytokines and participate in the onset of apoptosis.[5,6] It has been reported that up-regulation of JNK activity is associated with a number of disease states such as type-2 diabetes, obesity, cancer, inflammation, and stroke.[1–3] Therefore, JNK inhibitors are expected to be effective therapeutic agents against a variety of diseases.

JNKs bind to substrates and scaffold proteins, such as JIP-1, that contain a D-domain, as defined by the consensus sequence R/KXXXXLXL.[7,8] A peptide corresponding to the D-domain of JIP-1 (aa 153–163; pep-JIP1), inhibits JNK activity in vitro and displays noteworthy selectivity with little inhibition of the closely related Erk and p38 MAPKs.[9–12] Recent in vivo data, generated for studies focusing on pep-JIP1 fused to the cell permeable HIV-TAT peptide, show that its administration in various mice models of insulin resistance and type-2 diabetes restores normoglycemia without causing hypoglycemia.[13] Despite these encouraging data, peptide's instability in vivo may hamper the development on novel JNK-related therapies based on such peptides.[9–13]

Hence, there has been considerable effort to identify small molecule JNK inhibitors over the past several years.[14–22] A drug discovery program in our laboratory was initiated with the aim of identifying and characterizing small molecule JNK inhibitors as novel chemical entities targeting its JIP binding site rather then the highly conserved ATP binding site of the protein. Very recently, we have reported the identification of 5-(5-nitrothiazol-2-ylthio)-1,3,4-thiadiazol-2-amine series[20] related to compound **BI-78D3**[19] (Fig. 1), as initial JIP mimetic inhibitors. These compounds were discovered using a displacement assay with a biotinylated-pepJIP1 peptide and employing a DELFIA assay platform (Section 2) in a medium size screening campaign.[19] In our continued interest in the development of JNK inhibitors,[18–21] we now report further structure activity relationship studies describing novel small molecules thiadiazole derivatives as JNK inhibitors targeting its JIP/substrate docking site.

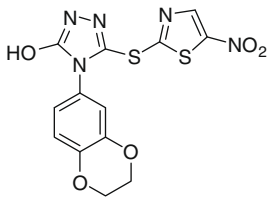

BI-78D3

Figure 1. Chemical structures of pepJIP1 based tool compounds previously reported from our lab.

* Corresponding author. Tel.: +1 858 646 3159; fax: +1 858 713 9925.
E-mail address: mpellecchia@burnham.org (M. Pellecchia).

0968-0896/$ - see front matter © 2009 Elsevier Ltd. All rights reserved.
doi:10.1016/j.bmc.2009.12.013

Recent work from our laboratory demonstrates that compound **BI-78D3** (Fig. 1) served as a useful tool compound for understanding the consequences of JNK substrate competitive inhibitors in vitro and in vivo; however, the compound lacked many chemical features considered desirable in a clinical candidate, including plasma stability. Moreover, it is possible that the compound may covalently bind to a surface exposed Cys residue, located at the center of the JIP binding groove.[19] Hence, in our continued search for a JNK inhibitor suitable for clinical studies, we report on a thiadiazole series and focused on improved cellular potency, solubility, cell permeability and plasma stability.

The general synthetic routes utilized thiols (**3**, Scheme 1) that were either synthesized according to previously reported procedures,[23,24] or that were commercially available from Enamine (Ukraine). Final compounds (**4, BI-90B5**–**BI-90H10,** Table 1 and Supplementary data) were synthesized by nucleophilic substitution of 2-bromo-5-nitrothiazole with the corresponding thiols of thiadiazoles in the presence of NaOMe in methanol at room temperature (Section 2). Initially, we synthesized several analogs of aryl derivatives of thiadiazoles (**BI-90B5, 90B7, 90D8, 90D7, 90D8**, **90D10, 90E1, 90E6, 90E9,** and **90F2,** see in Supplementary data) but none of these resulted in compound with appreciable inhibition of JNK in a kinase activity assay, although some compounds displayed a significant ability to displace pepJIP1 in a DELFIA assay. Our explanation is that the small nature of our test compounds may result in different binding modes along the extended JIP binding groove. We can only speculate that compounds that displace pepJIP1 by binding on the JIP surface occupied by the conserved LXL motif, in closer proximity to the ATP site, may result more effective kinase inhibitors. We therefore decided to focus on the benzylthiadiazole series. We observed that a 4-methoxybenzyl (**BI-90H8**) showed better activity than a simple benzyl derivative (**BI-90E2**). We subsequently found that compounds of the alkylthiadiazole series had improved activities in both assays although the bulkier *tert*-butyl (**BI-90E7**), cyclopropyl, and cyclohexyl groups (Supplementary data) were not tolerated on 2-position of thiadiazole series suggesting steric hindrance with the target. Interestingly, substituting in the 2-position with either an ethyl group (**BI-90G12**) or an *n*-butyl group (**BI-90H4**) resulted in compounds with limited activity. However, when the substituent in 2-position is a 2-methoxyethyl group (**BI-90H9**), sec-butyl group (**BI-98A10**), and *n*-propyl group (**BI-90H6**) these lead to compounds with improved activity in both the pepJIP1 displacement (DELFIA) and the kinase activity (LANTHA) assays. Of these compounds, **BI-90H9** showed an IC_{50} of 4.8 μM in the kinase assay (Fig. 2A) in a substrate competitive manner and accordingly it displaced pepJIP1 with an IC_{50} of 158 nM (Fig. 2B). Furthermore, compound **BI-90H9** was found to be 20 times less active (Table 2) against p38α, a member of the MAPK family with high structural similarity to JNK, and practically inactive against the kinase Akt. These compounds were also inactive against other unrelated proteins under investigation in our laboratory, including metallo-proteases such as anthrax lethal factor, and a serin protease (furin) (Table 2), further corroborating that these compounds may selectively interfere with the JNK docking site. This selectivity is in agreement with our previous findings with compound **BI-78D3**[19] (Fig. 1) and with the reported data on pepJIP1.[9–13]

Previous modeling studies,[18,19] supported by NMR relaxation measurements, suggest that compound **BI-78D3** may bind at the JIP site with the nitrothiazole group crossing the ridge close to residue Cys163 (Fig. 3A). Its benzo-dioxane group occupies the deep hydrophobic pocket along the JIP binding groove, occupied by the side chains of the essential Leu residues of the R/KXXXXLXL binding motif in pepJIP1. In such docked conformation, the compound brings the thio-ether atom in proximity to a surface exposed Cys residue in the JIP1 binding groove (Fig. 3A). Previous ITC measurements with compound **BI-78D3** and a single point C163S JNK2 mutant suggested a possible involvement of this residue in the binding properties of the compound.[19] Interestingly, docking studies with compound **BI-90H9** suggest that the compound protrudes its methoxy group into the JIP binding groove occupied by the Leu residues of pepJIP1, and that the thiadiazole group can form hydrogen bonds with protein backbone atoms (Fig. 3B). In agreement with this docked pose and the observed SAR, the length of the side chain at the 2-position is critical to properly locate the thiadiazole to form hydrogen bonding interactions and to fully occupy the Leu binding pocket (Fig. 3B). Moreover, in this docking pose, the thioether of **BI-90H9** is far from the side chain of Cys163, hence its binding properties should not be dependent on this residue. Accordingly, ITC measurements with a C163S JNK2 mutant reveal that the compound binding to this mutant with a dissociation constant K_d of 4.2 μM (Fig. 2C) versus 2.8 μM obtained against wt-JNK2, whereas compound **BI-78D3** showed over 50-fold reduction in binding affinity to the mutant.[19]

In an attempt to further profile the properties of compound **BI-90H9** in the context of a complex cellular milieu, we employed the cell-based LanthaScreen™ kinase assay. In this assay platform, compound **BI-90H9** is able to inhibit TNF-α stimulated phosphorylation of c-Jun (IC_{50} = 8 μM). We also tested some other compounds on the cell based assay, among them **BI-90H9** showed the most cellular activities (IC_{50} values for **BI-90H8,** and **BI-98A10** were 21 μM, and 20 μM, respectively). It should be noted that the cell-based system employed makes use of a GFP-c-Jun stable expression system. As a result, the levels of GFP-c-Jun in these cells are higher than endogenous levels. This could have an inflationary effect on the IC_{50} values obtained with this assay when

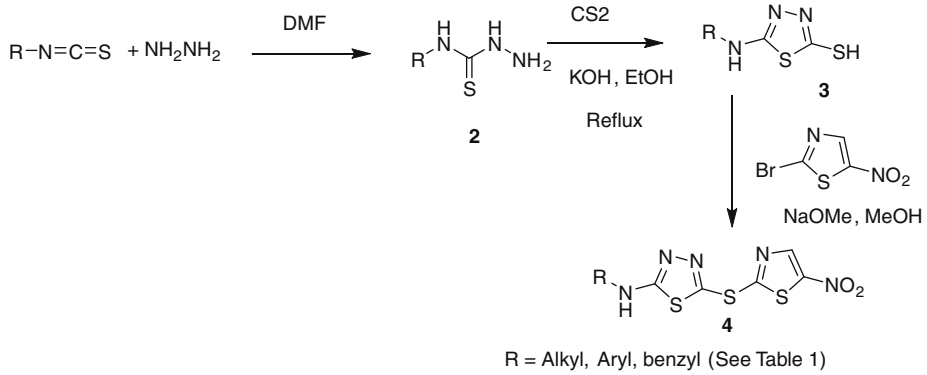

Scheme 1. Synthetic scheme used to prepare the thiadiazole derivatives reported in Table 1.

Table 1
Inhibition results for thiadiazole derivatives against JNK

Compound	ID	IC_{50}[a] (μM)	IC_{50}[b] (μM)	LE[c]
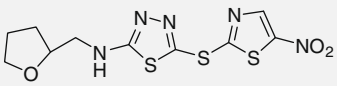	**BI-90H5**	10	0.47	0.32
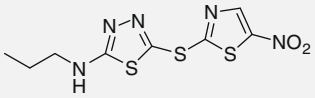	**BI-90H6**	6.7	0.29	0.39
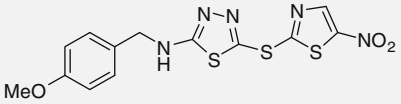	**BI-90H8**	9.1	0.10	0.23
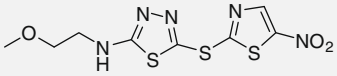	**BI-90H9**	4.8	0.16	0.38
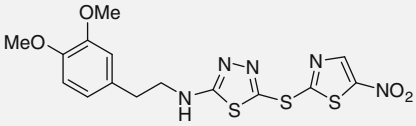	**BI-90H10**	5.7	0.10	0.26
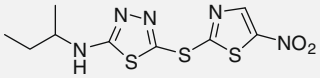	**BI-98A10**	3.0	0.14	0.39
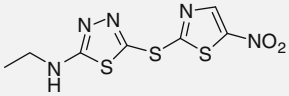	**BI-90G12**	~100	10	0.32
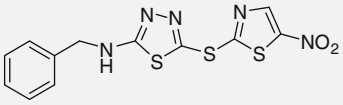	**BI-90E2**	[d]	[d]	[d]
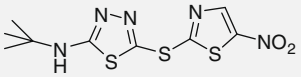	**BI-90E7**	[d]	[d]	[d]
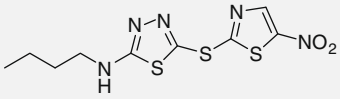	**BI-90H4**	[d]	[d]	[d]
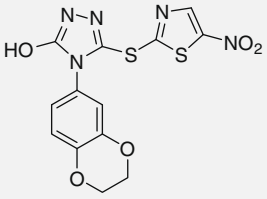	**BI-78D3**	0.28	0.50	0.36

[a] JNK1 kinase inhibition assay (LANTHA); values are means of at least three or more experiments.
[b] pepJIP1 displacement assay (DELFIA); values are means of at least three or more experiments.
[c] Ligand efficiency was calculated based on the kinase activity inhibition data.[30,31]
[d] These compounds did not show a significant inhibition in the kinase assay up to 25 μM, although showed some activity (~20%) in displacing pepJIP1 in DELFIA assay at 50 μM.

testing substrate competitive compounds. Nonetheless, this finding establishes that compound **BI-90H9** is able to function in a cellular context and that its activity parallels the in vitro findings.

Finally, liquid chromatography/mass spectrometry bio-availability analysis (see Section 2) demonstrated that compound **BI-90H9** had favorable plasma stability (68% remaining after 60 min in plasma stability analysis) and cell permeability, improving upon our previous lead molecule, **BI-78D3** (Table 3). We observed that a simple *n*-propyl group (**BI-90H6**) and 3,4-dimethoxyphenethyl group (**BI-90H10**) in 2-position of 1,3,4-thiadiazole derivatives degraded rapidly after 1 h of incubation in rat plasma (Table 3 and Supplementary data). These results suggested that a 2-methoxyethyl group on 2-position of thiadiazole (**BI-90H9**) is the most suitable group for improving plasma stability.

In summary, compound **BI-90H9** can be considered to have a good balance of potency, selectivity, solubility, cellular activity, and plasma stability. These data and the binding mode of the compound provide a solid basis for further optimizations. For example, the predicted proximity of the compound to the ATP site suggests that it may be possible to obtain bi-dentate molecules spanning both sites.[18] We are currently exploring this possibility. Nonetheless, our results indicate once more that targeting the protein JIP docking site with a small molecule is a novel and promising avenue for the development of protein kinase related therapeutics.

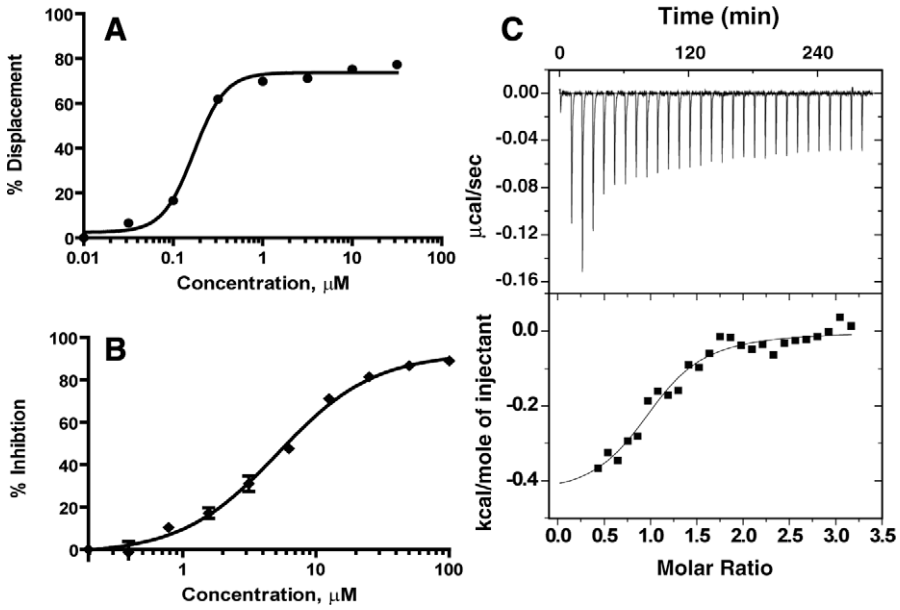

Figure 2. In vitro activity of compound BI-90H9. (A) Dose–response curve for the in vitro inhibition of the kinase activity JNK1 by BI-90H9 using GFP-c-Jun as substrate (LANTHA assay platform). (B) Dose–dependent curve for the in vitro displacement of biotinylated pep-JIP1 from GST-JNK1 (DELFIA assay platform).

Table 2
Selectivity profile

Compound	JNK1, IC_{50} (μM)	p-38α , IC_{50} (μM)	Akt, IC_{50} (μM)	Furin, IC_{50} (μM)	LF, IC_{50} (μM)
BI-90H6	6.7	>100	>100	>50	>100
BI-90H9	4.8	>100	>100	>50	>100
BI-90H10	5.7	>100	>100	>50	>100
BI-98A10	3.0	>100	>100	>50	>100

Table 3
Plasma and cell permeability data

Compound	Plasma stability	Cell permeability, PAMPA % flux[a]
BI-78D3	42% remaining after 60 min	30
BI-90H6	35% remaining after 60 min	49.8
BI-90H9	68% remaining after 60 min	76.3
BI-90H10	0% remaining after 60 min	5.5

[a] Flux values: <5% low permeation; 5–30% medium permeation; 30–100% high permeation.

2. Experimental

2.1. General

Unless otherwise indicated, all anhydrous solvents were commercially obtained and stored in Sure-seal bottles under nitrogen. All other reagents and solvents were purchased as the highest grade available and used without further purification. Thin-layer chromatography (TLC) analysis of reaction mixtures was performed using Merck Silica Gel 60 F254 TLC plates, and visualized using ultraviolet light. NMR spectra were recorded on Varian 300 or 500 MHz instruments. Chemical shifts (δ) are reported in parts per million (ppm) referenced to ^1H (Me_4Si at 0.00). Coupling constants (J) are reported in Hz throughout. Mass spectral data were acquired on Shimadzu LC–MS-2010EV for low resolution, and on an Agilent ESI-TOF for either high or low resolution. Purity of all compounds was obtained in a HPLC Breeze from Waters Co. using an Atlantis T3 3 μm 4.6 × 150 mm reverse phase column. The eluant was a linear gradient with a flow rate of 1 mL/min from 95% A and 5% B to 5% A and 95% B in 15 min followed by 5 min at 100% B (solvent A: H_2O with 0.1% TFA; Solvent B: ACN with 0.1% TFA). The compounds were detected at λ = 254 nm. Purity of key compounds was established by elemental analysis as performed on a Perkin–Elmer series II-2400. Combustion analysis was performed by Nu-Mega Resonance labs, Inc., San Diego, CA.

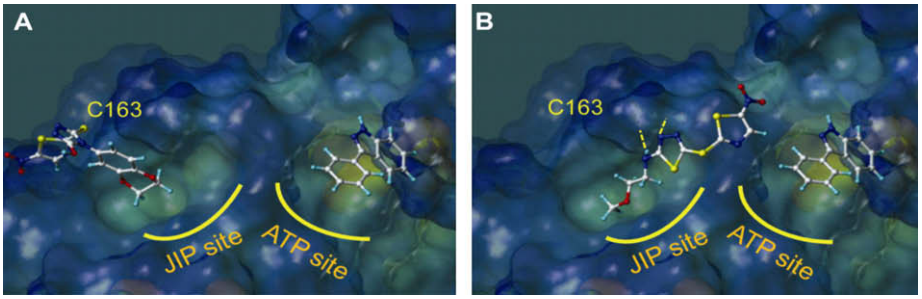

Figure 3. Molecular docking studies. Surface representation of JNK1 *** (PDB ID 1UKI) with docked compounds occupying the JIP binding site and the ATP site as indicated. The position of residue Cys163 is indicated. In A) the compound **BI-78D3** (on the left) and an ATP mimetic compound (on the right) are reported. In B), the compound **BI-90H9** (on the left) and the same ATP mimetic (on the right) are reported. Intermolecular hydrogen bonding interactions are depicted as dashed yellow lines.

2.2. Synthesis of *N*-(2-methoxyethyl)-5-(5-nitrothiazol-2-ylthio)-1,3,4-thiadiazol-2-amine (BI-90H9)

To a solution of 5-(2-methoxyethylamino)-1,3,4-thiadiazole-2-thiol (100 mg, 0.523 mmol) in MeOH (3 mL) was added MeONa (1.25 mL, 0.5 M solution in MeOH) and stirred. After 5 min, 2-bromo-5-nitrothiazole (119 mg, 0.575 mmol) was added to the reaction mixture and stirred at room temperature until deemed complete by TLC (16 h). The reaction mixture was acidified with 1 N HCl and the resulting precipitate was collected by filtration and washed with water (2 × 30 mL), haxanes (2 × 30 mL), and 10% ethyl acetate in hexanes (2 × 30 mL) to give a white solid. The residue was chromatographed over silica gel (70% ethyl acetate in hexane) to afford the **BI-90H9** (118 mg, 71%). ^{1}H NMR (300 MHz, DMSO-d_6) δ 3.24–3.30 (m, 2H), 3.32 (s, 3H), 3.46–3.57 (m, 2H), 8.47 (t, J = 5.4 Hz, 1H, NH), 8.75 (s, 1H); MS *m/z* 341 $(M+Na)^+$, 319 $(M+H)^+$, 217, 171, 147, 138, 125, 106, 102, 97, 84; HRMS calcd for $C_8H_{10}N_5O_3S_3$ (M+H) 319.9940, found 319.9945. Anal. calcd for $C_8H_9N_5O_3S_3$: C, 30.08; H, 2.84; N, 21.93; S, 30.12. Found: C, 30.16; H, 2.95; N, 21.80; S, 30.01.

Following above mentioned procedure (**BI-90H9**) and the appropriate starting materials and reagents used; compounds (**BI-90B7–90H10** and **BI-98A10**) were synthesized.

2.2.1. *N*-Ethyl-5-(5-nitrothiazol-2-ylthio)-1,3,4-thiadiazol-2-amine (BI-90G12)

Yield: 62% ; ^{1}H NMR (300 MHz, DMSO-d_6) δ 1.20 (t, J = 6.5 Hz, 3H), 3.31 (quintet, J = 6.5 Hz, 2H), 8.41 (s, 1H), 8.75 (t, J = 5.4 Hz, 1H, NH); MS *m/z* 311 $(M+Na)^+$, 289 $(M+H)^+$, 204, 190, 138, 106, 102, 84; HRMS calcd for $C_7H_8N_5O_2S_3$ (M+H) 289.9835, found: 289.9839.

2.2.2. 5-(5-Nitrothiazol-2-ylthio)-*N*-((tetrahydrofuran-2-yl)methyl)-1,3,4-thiadiazol-2-amine (BI-90H5)

Yield: 41%; ^{1}H NMR (300 MHz, DMSO-d_6) δ 1.50–1.65 (m, 2H), 1.80–2.00 (m, 2H), 3.65 (q, J = 6.9 Hz, 2H), 3.78 (q, J = 7.8 Hz, 2H), 4.03 (sextet, J = 4.5 Hz, 1H), 8.48 (t, J = 6 Hz, NH), 8.74 (s, 1H); MS *m/z* 346 $(M+H)^+$, 158, 147, 121, 110, 102, 100, 84; HRMS calcd for $C_{10}H_{12}N_5O_3S_3$ (M+H) 346.0097, found 346.0100.

2.2.3. 5-(5-Nitrothiazol-2-ylthio)-*N*-propyl-1,3,4-thiadiazol-2-amine (BI-90H6)

Yield: 60% ; ^{1}H NMR (300 MHz, DMSO-d_6) δ 0.93 (t, J = 7.8 Hz, 3H), 1.61 (sextet, J = 7.2 Hz, 2H), 3.29 (q, J = 7.2 Hz, 2H), 8.43 (t, J = 5.4 Hz, 1H, NH), 8.75 (s, 1H); MS *m/z* 325 $(M+Na)^+$, 303 $(M+H)^+$, 204, 190, 138, 126, 106, 102, 84; HRMS calcd for $C_8H_{10}N_5O_2S_3$ (M+H) 303.9991, found: 303.9996.

2.2.4. *N*-(4-Methoxybenzyl)-5-(5-nitrothiazol-2-ylthio)-1,3,4-thiadiazol-2-amine (BI-90H8)

Yield: 29%; ^{1}H NMR (300 MHz, DMSO-d_6) δ 3.74 (s, 3H), 4.48 (d, J = 5.4 Hz, 2H), 6.92 (d, J = 7.8 Hz, 2H), 7.31 (d, J = 7.8 Hz, 2H), 8.74 (s, 1H), 8.81 (s, NH); MS *m/z* 403 $(M+Na)^+$, 382 $(M+H)^+$, 359, 349, 316, 185, 147, 132, 105, 100, 90, 64; HRMS calcd for $C_{13}H_{12}N_5O_3S_3$ (M+H) 382.0097, found: 382.0095.

2.2.5. *N*-(2-Methoxyethyl)-5-(5-nitrothiazol-2-ylthio)-1,3,4-thiadiazol-2-amine (BI-90H9)

Yield: 71%; ^{1}H NMR (300 MHz, DMSO-d_6) δ 3.24–3.30 (m, 2H), 3.32 (s, 3H), 3.46–3.57 (m, 2H), 8.47 (t, J = 5.4 Hz, 1H, NH), 8.75 (s, 1H); MS *m/z* 341 $(M+Na)^+$, 319 $(M+H)^+$, 217, 171, 147, 138, 125, 106, 102, 97, 84; HRMS calcd for $C_8H_{10}N_5O_3S_3$ (M+H) 319.9940, found 319.9945. Anal. calcd for $C_8H_9N_5O_3S_3$: C, 30.08; H, 2.84; N, 21.93; S, 30.12. Found: C, 30.16; H, 2.95; N, 21.80; S, 30.01.

2.2.6. *N*-(3,4-Dimethoxyphenethyl)-5-(5-nitrothiazol-2-ylthio)-1,3,4-thiadiazol-2-amine (BI-90H10)

Yield: 49%; ^{1}H NMR (300 MHz, DMSO-d_6) δ 2.84 (t, J = 6.75, 2H), 3.58 (q, J = 6.0 Hz, 2H), 3.70 (s, 3H), 3.73 (s, 3H), 6.76 (d, J = 8.7 Hz, 1H), 6.85–6.90 (m, 2H), 8.44 (t, J = 6 Hz, NH), 8.77 (s, 1H); MS *m/z* 448 $(M+Na)^+$, 426 $(M+H)^+$, HRMS calcd for $C_{15}H_{16}N_5O_4S_3$ (M+H) 426.0359, found: 426.0359.

2.2.7. *N*-sec-Butyl-5-(5-nitrothiazol-2-ylthio)-1,3,4-thiadiazol-2-amine (BI-98A10)

Yield: 64%; ^{1}H NMR (300 MHz, DMSO-d_6) δ 0.91 (t, J = 7.5 Hz, 3H), 1.19 (d, J = 6.6 Hz, 3H), 1.56 (quintet, J = 7.5 Hz, 2H), 3.71–3.79 (m, 1H), 8.32 (d, J = 6.2 Hz, 1H, NH), 8.75 (s, 1H); MS *m/z* 339 $(M+Na)^+$, 318 $(M+H)^+$, 252, 226, 158, 147, 138, 106, 84; HRMS calcd for $C_9H_{12}N_5O_2S_3$ (M+H) 318.0148, found: 318.0147.

2.3. Plasma stability assay

Briefly, each test compound solution was incubated (1 μM, 2.5% final DMSO concentration) with fresh rat plasma at 37 °C. The reactions were terminated at 0, 30, and 60 min by the addition of two volumes of methanol containing internal standard. Following protein precipitation and centrifugation, the samples were analyzed by LC–MS. The percentage of parent compound remaining at each time point relative to the 0 min sample is calculated from peak area ratios in relation to the internal standard. Compounds were run in duplicate with a positive control known to be degraded in plasma.

2.4. PAMPA permeability assay

PAMPA is an in vitro model of passive, transcellular permeation useful for ranking compounds based on their potential to cross cell membranes and the gastrointestinal wall.

A 96-well microtiter plate completely filled with aqueous buffer solutions (pH 7.4) is covered with a microtiter filterplate in a sort of sandwich construction. The hydrophobic filter material (Durapore/Millipore; pore size 0.22–0.45 m) of wells (sample) of the filterplate is impregnated with a 1–20% solution of phospholipid in an organic solvent (Avanti Polar Lipids). Transport studies were started by the transfer of 100–200 μL of a 20 μM stock solution on top of the filterplate in the sample and in the reference section, respectively. An equilibrium plate (compounds at the theoretical equilibrium, that is, the resulting concentration if the donor and the acceptor solutions are combined) was also created and analyzed. This Acceptor plate and equilibrium plate concentrations were used to calculate the percentage of permeation (flux) of the compounds. The maximum DMSO content of the stock solutions was <2%. The PAMPA % flux was 76.3% for **BI-90H9** indicated high permeation (Table 3). Reference compounds were included and reported as Supplementary data.

2.5. DELFIA assay (dissociation enhanced lanthanide fluoro-immuno assay)

To each well of 96-well streptavidin-coated plates (Perkin–Elmer) 100 μL of a 100 ng/mL solution of biotin-labeled pep-JIP11 (Biotin-lc-KRPKRPTTLNLF, where lc indicates a hydrocarbon chain of six methylene groups) was added. After 1-h incubation and elimination of unbound biotin-pep-JIP11 by three washing steps, 87 μL of Eu-labeled anti-GST antibody solution (300 ng/mL; 1.9 nM), 2.5 μL DMSO solution containing test compound, and 10 μL solution of GST-JNK2 for a final protein concentration of 10 nM was added. After 1 h incubation at 0 °C, each well was washed five times to eliminate unbound protein and the Eu-antibody if displaced by a test compound. Subsequently, 200 μL of

enhancement solution (Perkin–Elmer) was added to each well and fluorescence measured after 10 min incubation (excitation wavelength, 340 nm; emission wavelength, 615 nm). Controls include unlabeled peptide and blanks receiving no compounds. Protein and peptide solutions were prepared in DELFIA buffer (Perkin–Elmer).

2.6. In vitro kinase assay

The LanthaScreen™ assay platform from Invitrogen was utilized. The time-resolved fluorescence resonance energy transfer assay (TR-FRET) was performed in 384 well plates. Each well received JNK1 (35 ng/mL, JNK1 MW = 45 KDa), ATF2 (400 nM), and ATP (0.2 μM) in 50 mM HEPES, 10 mM $MgCl_2$, 1 mM EGTA and 0.01% Brij-35, pH 7.5 and test compounds. The kinase reaction was performed at room temperature for 1 h. After which, the terbium labeled antibody and EDTA were added into each well. After an additional hour incubation, the signal was measured at 520/495 nm emission ratio on a fluorescence plate reader (Victor 2, Perkin–Elmer).

2.7. Cell based assays for c-Jun phosphorylation

The cell based kinase assays for c-Jun and ATF2 phosphorylation were carried out using the LanthaScreen c-Jun (1–79) Hela (Invitrogen, Carlsbad, CA) which stably express GFP-c-Jun 1–79. Phosphorylation was determined by measuring the time-resolved FRET (TR-FRET) between a terbium labeled phospho-specific antibody and the GFP-fusion protein.[12] The cells were plated in white tissue culture treated 384 well plates at a density of 10000 cell per well in 32 μL assay medium (Opti-MEM®, supplemented with 1% charcoal/dextran-treated FBS, 100 U/mL penicillin and 100 μg/mL streptomycin, 0.1 mM non-essential amino acids, 1 mM sodium pyruvate, 25 mM HEPES pH 7.3, and lacking phenol red). After overnight incubation, cells were pretreated for 60 min with compound (indicated concentration) followed by 30 min of stimulation with 2 ng/mL of TNF-alpha which stimulates both JNK and p38. The medium was then removed by aspiration and the cells were lysed by adding 20 μL of lysis buffer (20 mM Tris–HCl pH 7.6, 5 mM EDTA, 1% NP-40 substitute, 5 mM NaF, 150 mM NaCl, 1:100 protease and phosphatase inhibitor mix, SIGMA P8340 and P2850, respectively). The lysis buffer included 2 nM of the terbium labeled anti-pc-Jun (pSer73) detection antibodies (invitrogen). After allowing the assay to equilibrate for 1 h at room temperature, TR-FRET emission ratios were determined on a BMG Pherastar fluorescence plate reader (excitation at 340 nm, emission 520 nm and 490 nm; 100 μs lag time, 200 μs integration time, emission ratio = Em520/Em 490).

2.8. Isothermal titration calorimetry

Titrations were done using a VP-ITC calorimeter from Microcal (Northampton, MA). C163S JNK2 and wt-JNK2 were used at 50 μM in 20 mM sodium phosphate buffer (pH 7.4), 5% DMSO, and 0.01% triton X-100. Titrants were used at 750 μM in the same buffer. Titrations were carried out at 25 °C. Data were analyzed using Microcal Origin software provided by the ITC manufacturer (Microcal, Northampton, MA).

2.9. Molecular modeling

Molecular modeling studies were conducted on a Linux workstation and a 64 3.2-GHz CPUs Linux cluster. Docking studies were performed using the X-ray coordinates of JNK1 (PDB code 1UKH).[21,25] The complexed JIP peptide and ATO mimetic compound SP600125 were extracted from the protein structure and was used to define the binding site for docking of small molecules. The docked geometry of the indazole ATP mimetic reported in Figure 3 was simply derived from the X-ray coordinates of the parent compound, SP600125. The genetic algorithm (GA) procedure in the GOLD docking software performed flexible docking of small molecules whereas the protein structure was static.[25–29] For each compound, 20 solutions were generated and subsequently ranked according to Chemscore.[25] The protein surface was prepared with the program MOLCAD as implemented in Sybyl and was used to analyze the binding poses for studied small molecules.[25–29]

Acknowledgments

We gratefully acknowledge financial support from the NIH (Grants nos. DK073274 and DK080263) and Syndexa pharmaceuticals (to M.P.).

Supplementary data

Supplementary data associated with this article can be found, in the online version, at doi:10.1016/j.bmc.2009.12.013.

References

1. Manning, G. *Science* **2002**, *298*, 1912–1934.
2. Manning, A. M.; Davis, R. J. *Nat. Rev. Drug Disc.* **2003**, *2*, 554–565.
3. Bogoyevitch, M. A.; Arthur, P. G. *Biochim. Biophys. Acta* **2008**, *1784*, 76–93. and references cited therein.
4. Gupta, S.; Barrett, T.; Whitmarsh, A. J.; Cavanagh, J.; Sluss, H. K.; Dérijard, B.; Davis, R. J. *EMBO J* **1996**, *15*, 2760–2770.
5. Kyriakis, J. M.; Avruch, J. *Physiol. Rev.* **2001**, *81*, 807–869.
6. Pearson, G.; Robinson, R.; Gibson, T. B.; Xu, B. E.; Karandikar, M.; Berman, K.; Cobb, M. H. *Endocr. Rev.* **2001**, *22*, 153–183.
7. Kallunki, T.; Deng, T.; Hibi, M.; Karin, M. *Cell* **1996**, *87*, 929–939.
8. Yang, S.-H.; Whitmarsh, A. J.; Davis, R. J.; Sharrocks, A. D. *EMBO J* **1998**, *17*, 1740–1749.
9. Barr, R. K.; Kendrick, T. S.; Bogoyevitch, M. A. *J. Biol. Chem.* **2002**, *277*, 10987–10997.
10. Bonny, C.; Oberson, A.; Negri, S.; Sauser, C.; Schorderet, D. F. *Diabetes* **2001**, *50*, 77–82.
11. Dickens, M.; Roger, J. S.; Cavanagh, J.; Raitano, A.; Xia, Z.; Halpern, J. R.; Greenberg, M. E.; Sawyers, C. L.; Davis, R. J. *Science* **1997**, *277*, 693–696.
12. Heo, Y.-S.; Kim, S.-K.; Seo, C. I.; Kim, Y.-K.; Sung, B.-J.; Lee, H. S.; Lee, J. I.; Park, S.-Y.; Kim, J. H.; Hwang, K. Y.; Hyun, Y.-L.; Jeon, Y. H.; Ro, S.; Cho, J. M.; Lee, T. G.; Yang, C.-H. *EMBO J* **2004**, *23*, 2185–2195.
13. Kaneto, H.; Nakatani, Y.; Miyatsuka, T.; Kawamori, D.; Matsuoka, T.; Matsuhisa, M.; Kajimoto, Y.; Ichijo, H.; Yamasaki, Y.; Hori, M. *Nat. Med.* **2004**, *10*, 1128–1132.
14. Shin, Y.; Chen, W.; Habel, J.; Duckett, D.; Ling, Y. Y.; Koenig, M.; He, Y.; Vojkosvsky, T.; LoGrasso, P.; Kamenecka, T. M. *Bioorg. Med. Chem. Lett.* **2009**, *19*, 3344–3347. and references cited therein.
15. Gaillard, P.; Jeanclaude-Etter, I.; Ardissone, V.; Arkinstall, S.; Cambet, Y.; Camps, M.; Chabert, C.; Church, D.; Cirillo, R.; Gretener, D.; Halazy, S.; Nichols, A.; Szyndralewiez, C.; Vitte, P.-A.; Gotteland, J.-P. *J. Med. Chem.* **2005**, *48*, 4596–4607.
16. Rückle, T.; Biamonte, M.; Grippi-Vallotton, T.; Arkinstall, S.; Cambet, Y.; Camps, M.; Chabert, C.; Church, D. J.; Halazy, S.; Jiang, X.; Martinou, I.; Nichols, A.; Sauer, W.; Gotteland, J.-P. *J. Med. Chem.* **2004**, *47*, 6921–6934.
17. Bennett, B. L.; Sasaki, D. T.; Murray, B. W.; O'Leary, E. C.; Sakata, S. T.; Xu, W.; Leisten, J. C.; Motiwala, A.; Pierce, S.; Satoh, Y.; Bhagwat, S. S.; Manning, A. M.; Anderson, D. W. *Proc. Natl. Acad. Sci.* **2001**, *98*, 13681–13686.
18. Vazquez, J.; De, S. K.; Chen, L.-H.; Riel-Mehan, M.; Emdadi, A.; Cellitti, J.; Stebbins, J. L.; Rega, M. F.; Pellecchia, M. *J. Med. Chem.* **2008**, *51*, 3460–3465.
19. Stebbins, J. L.; De, S. K.; Machleidt, T.; Becattini, B.; Vazquez, J.; Kuntzen, C.; Chen, L.-H.; Cellitti, J. F.; Riel-Mehan, M.; Emdadi, A.; Solinas, G.; Karin, M.; Pellecchia, M. *Proc. Natl. Acad. Sci.* **2008**, *105*, 16809–16813.
20. De, S. K.; Stebbins, J. L.; Chen, L.-H.; Riel-Mehan, M.; Machleidt, T.; Dahl, R.; Yuan, H.; Emdadi, A.; Barile, E.; Chen, V.; Murphy, R.; Pellecchia, M. *J. Med. Chem.* **2009**, *52*, 1943–1952.
21. Zhao, H.; Serby, M. D.; Xin, Z.; Szczepankiewicz, B. G.; Liu, M.; Kosogof, C.; Liu, B.; Nelson, L. T. J.; Johnson, E. F.; Wang, S.; Pederson, T.; Gum, R. J.; Clampit, J. E.; Haasch, D. L.; Abad-Zapatero, C.; Fry, E. H.; Rondinone, C.; Trevillyan, J. M.; Sham, H. L.; Liu, G. *J. Med. Chem.* **2006**, *49*, 4455–4458.
22. Chen, T.; Kablauoi, N.; Little, J.; Timofeevski, S.; Tschantz, W. R.; Chen, P.; Peng, J.; Charlton, M.; Stanton, R.; Bauer, P. *Biochem. J.* **2009**, *420*, 283–294.
23. Chu, C.-H.; Hui, X.-P.; Xu, P.-F.; Zhang, Z.-Y.; Li, Z.-C.; Lioa, R.-A. *Indian J. Chem.* **2002**, *41B*, 2436–2438.

24. Raphael, E.; Joshua, C. P.; Koshy, L. *Indian J. Chem.* **1989**, *28B*, 635–638.
25. GOLD, Version, 2.1; The Cambridge Crystallographic Data Centre: 12, Union Road, Cambridge, CB2 1EZ, UK.
26. Jones, G.; Willett, P.; Glen, R. C.; Leach, A. R.; Taylor, R. *J. Mol. Biol.* **1997**, *267*, 727–748.
27. Eldridge, M. D.; Murray, C. W.; Auton, T. R.; Paolini, G. V.; Mee, R. P. *J. Comput. Aided Mol. Des.* **1997**, *11*, 425–455.
28. Teschner, M.; Henn, C.; Volhardt, H.; Reiling, S.; Brickmann, J. *J. Mol. Graphics* **1994**, *12*, 98–105.
29. Pearlman, R. S. "Concord," distributed by Tripos International, St. Louis, Missouri, 63144, USA.
30. Hopkins, A. L.; Groom, C. R.; Alex, A. *Drug Discovery Today* **2004**, *9*, 430–431.
31. Kuntz, I. D.; Chen, K.; Sharp, K. A.; Kollman, P. A. *Proc. Natl. Acad. Sci. U.S.A.* **1999**, *96*, 9997–10002.